Strand dependent bypass of DNA lesions during fork reversal by ATP-dependent translocases SMARCAL1, ZRANB3, and HLTF

Madison B. Adolph[1,2], Garrett M. Warren[4,5], Frank B. Couch[1,3], Briana H. Greer[4], Brandt F. Eichman[1,4,*], David Cortez[1,*]

[1]Department of Biochemistry, Vanderbilt University School of Medicine, Nashville, TN 37232

[2]Present Address: Department of Biochemistry and Molecular Biology, Saint Louis School of Medicine, St. Louis MO 63104

[3]Present Address: Twin Sun LLC, Nashville TN 37203

[4]Department of Biological Sciences, Vanderbilt University, Nashville, TN 37232

[5]Present Address: Molecular Biology Program, Sloan Kettering Institute, New York NY 10065

*corresponding authors: david.cortez@vanderbilt.edu and brandt.eichman@vanderbilt.edu

Running Title

DNA lesion sensitivities of fork reversal enzymes

Keywords

DNA replication, Replication stress, DNA damage, DNA damage response, DNA binding protein, HMCES, DNA-protein crosslink, DNA repair, abasic site, fork reversal

Abstract

During DNA replication, the replisome encounters obstacles including DNA lesions, transcription-replication conflicts, and other sources of replication stress. These obstacles must be efficiently overcome to complete DNA synthesis and minimize genome instability. One pathway to tolerate replication stress is replication fork reversal, in which parental template DNA strands are reannealed and a nascent-nascent DNA duplex is formed. Several enzymes promote replication fork reversal, including the ATP-dependent translocases SMARCAL1, ZRANB3, and HLTF. How these enzymes translocate on DNA that contains fork-stalling lesions is unknown. Here, we examined the abilities of SMARCAL1, ZRANB3, and HLTF to tolerate various lesions on leading or lagging template strands. We demonstrate that SMARCAL1 and ZRANB3 are selectively inhibited by lesions on the leading template strand, whereas HLTF is insensitive to bulky lesions on either strand. These results suggest that SMARCAL1 and ZRANB3 contact the leading strand during fork reversal and therefore are more sensitive to inhibition by bulky lesions on this strand. In contrast, HLTF DNA translocation is inherently insensitive to DNA lesions. These biochemical differences between the fork reversal enzymes provide insights into their mechanism of DNA remodeling and suggest they may act in lesion-specific contexts.

Introduction

To maintain genome stability, faithful and complete DNA replication must occur each cell division cycle despite challenges to DNA synthesis including DNA damage that stalls the replication machinery (1). Replication forks can encounter diverse types of DNA lesions, ranging from small base modifications and abasic sites to bulky DNA adducts like cyclobutane pyrimidine dimers and DNA protein crosslinks (DPCs). Stalling of the replication fork activates DNA damage response pathways and recruits DNA repair proteins (2,3). Prolonged or unresolved fork stalling results in hallmarks of genome instability such as cell cycle arrest, fork collapse, double-strand breaks, and loss of cell viability.

Multiple pathways exist to deal with stalled replication forks, including fork reversal, translesion synthesis (TLS), repriming, and template switching (2,4-7). While repriming and TLS have the propensity to induce mutations or other genome changes, fork reversal is thought to compete with repriming and TLS pathways to promote error-free bypass of lesions. Fork reversal converts the three-way DNA junction of the replication fork into a four-way, or Holliday-junction-like structure, through the annealing of the newly synthesized DNA strands and the reannealing of the parental strands. This process is mediated by fork reversal enzymes including the ATP-dependent translocases SMARCAL1, ZRANB3, HLTF (7-12).

SMARCAL1, ZRANB3, and HLTF are double-stranded DNA (dsDNA) translocases related to the Snf2 family of chromatin remodelers (13). Each contain a conserved ATP-dependent motor domain that enables dsDNA translocation and a unique substrate recognition domain (SRD) that provides specificity for fork structures (9,11,14,15). SMARCAL1 is recruited to replication forks by the single-stranded DNA (ssDNA) binding protein RPA (16-20), and contains two tandem HARP motifs that act as an SRD to recognize ssDNA/dsDNA junctions, likely by binding to the ssDNA exposed on template strands upon fork stalling and uncoupling (9,14). ZRANB3's

SRD also provides affinity for ssDNA/dsDNA junctions (15,21). However, the substrate preferences of SMARCAL1 and ZRANB3 are different (22). SMARCAL1 prefers model fork substrates with gaps on the leading strand and is stimulated when RPA is bound to this substrate, whereas ZRANB3 has no intrinsic preference and is inhibited by RPA on similar substrates (22,23). Similarly, HLTF does not have a preference for gaps on leading or lagging strands and is also inhibited by RPA (24). Unlike SMARCAL1 and ZRANB3, however, the HLTF substrate recognition (HIRAN) domain recognizes 3′ hydroxyl (3′OH) groups at ssDNA ends and is essential for fork reversal by binding to the 3′-end of the nascent leading strand (11,24-26).

As a protective mechanism, replication fork reversal may stabilize a stalled replication fork until a converging fork can replicate the region or promote a template switching mechanism by annealing the nascent DNA strands, allowing for synthesis past the lesion (7,8). Fork reversal also places the fork-stalling DNA lesion back into the context of duplex DNA where the lesion could then be repaired (7,8). The ability to place the lesion back into the context of duplex DNA may require that the fork reversal enzymes translocate through these lesions to generate the reversed fork. Whether fork reversal enzymes can translocate past DNA lesions is unknown. Here, we investigated the ability of SMARCAL1, ZRANB3, and HLTF to catalyze fork reversal when challenged by various lesions. We show that SMARCAL1 and ZRANB3 are strongly inhibited by bulky lesions on the leading strand template and are inhibited to a lesser extent by lesions on the lagging strand. Strikingly, HLTF is insensitive to lesions on either strand. This indicates that SMARCAL1 and ZRANB3 translocate similarly on model regression substrates and likely contact the leading strand template during the reversal process. HLTF is biochemically distinct from SMARCAL1 and ZRANB3 and can more robustly translocate through lesions on model replication fork substrates. These results highlight important functional differences among these enzymes and suggest they act in lesion-specific contexts.

Results

SMARCAL1 and ZRANB3 fork reversal activity is blocked by leading template strand Cy5 modifications

Based on previous studies suggesting there may be differences in how the SMARCAL1, ZRANB3, and HLTF enzymes translocate on DNA and remodel replication forks, we hypothesized that they could be differentially influenced by DNA lesions on the substrates. To test this idea, we asked if the enzymes would be differentially impeded by changes to the DNA backbone. We incorporated a Cy5 molecule internally between two phosphate groups of the DNA leaving a bulky fluorescent reporter protruding from the phosphodiester backbone (Figure S1). We placed the modification either on the leading or lagging template strand. When assembled into a fork structure, the modification is 5 nucleotides from the fork junction. We then tested how this modification alters the ability of SMARCAL1, ZRANB3, or HLTF to catalyze fork reversal. SMARCAL1 fork reversal activity is largely inhibited by the Cy5 modification when placed on the leading strand, but the lesion causes only a small reduction in activity when incorporated into the lagging strand (Figure 1A-B). Similarly, ZRANB3 activity is almost completely blocked when the lesion is on the leading strand but is only mildly inhibited by the modification on the lagging strand (Figure 1C-D). In contrast, HLTF is not inhibited when the Cy5 is placed on either strand (Figure 1E-F).

ZRANB3 and SMARCAL1 fork reversal activity is blocked by leading strand streptavidin-biotin lesions

To determine if these substrate preferences could extend to other DNA modifications including base alterations, we inserted a biotin group on a thymine residue in the leading or lagging template strand. In this case the modification was placed 20 nucleotides from the fork junction (Figure S1). After assembling the fork substrates, we added streptavidin to further increase the bulkiness of the model lesion. Similarly to the Cy5 modification, SMARCAL1 and ZRANB3 were

inhibited by the streptavidin-biotin moiety on the leading strand but retained most of their activity when the modification was on the lagging strand (Figure 2A-D). This inhibition is not due to the bulky lesion inhibiting binding to the substrate as these enzymes bind equally well (Supplemental Figure 1A-B). As seen with the Cy5 lesion, HLTF is not impeded by streptavidin-biotin lesions on either strand and can efficiently promote fork regression in the presence of the bulky lesion (Figure 2E-F). This is consistent with the activities observed with the Cy5 modification, indicating that either phosphodiester backbone or base modifications impede the enzymes similarly.

ZRANB3 and SMARCAL1 fork reversal activity is blocked by leading strand HMCES-DPCs

Finally, we sought to test if the strand specific inhibition of SMARCAL1 and ZRANB3 could be extended to a more physiologically relevant bulky lesion. One such bulky lesion is a HMCES-DNA protein crosslink (DPC). HMCES covalently crosslinks to ssDNA AP sites through a conserved SOS response-associated peptidase (SRAP) domain, generating a thiazolidine linkage (27-30). This DPC is thought to protect AP sites in ssDNA from AP endonucleases and error prone repair pathways (27). Self-reversal of the HMCES-DPC is stimulated by the formation of duplex DNA, which could be generated from fork reversal (31,32).

We first tested whether an AP site alone on the leading strand could impair translocation and found that none of the enzymes were inhibited (Figure 3). We then generated a HMCES-DPC on the ssDNA arm of a model replication fork substrate. We extended the length of the fork substrate to ensure that the region of ssDNA containing the AP site could be efficiently bound by HMCES to form a DPC (Figure S1). As seen with Cy5 and a streptavidin-biotin lesion, SMARCAL1 and ZRANB3 are selectively blocked when the HMCES-DPC is on the leading template strand (Figure 4A-D). Similar to the other conditions, the lesion on the lagging strand does not impair fork reversal to the same extent (Figure 4A-D). Again, this effect is the result of

inhibition of translocation and not reduced binding to the model substrate (Figure S2C-D). We were also interested if the size of the bulky lesion mattered for the selective inhibition of the fork reversal translocases. To that end, we proteolyzed the HMCES DPC so that there was a small peptide remaining. Interestingly, this peptide was not sufficient to impede fork reversal on the leading strand (Figure S3) indicating that DPC proteolysis could facilitate fork reversal.

Discussion

Our findings suggest that despite conservation in their ATPase domains, the fork remodeling enzymes SMARCAL1, ZRANB3, and HLTF have different mechanisms of fork reversal and translocation that may diversify cellular function. This work highlights that HLTF possesses a unique ability to translocate through bulky lesions, unlike SMARCAL1 and ZRANB3. SMARCAL1 and ZRANB3 are selectively inhibited by bulky lesions on the leading strand but not the lagging strand, suggesting that ZRANB3 shares a mechanism of dsDNA translocation with SMARCAL1. The different activities further explain why cells may need all three enzymes to promote fork reversal since a variety of DNA lesions can trigger fork reversal. The differences in their ability to translocate through strand-specific lesions, combined with other differences in substrate specificity may allow cells to deal with a variety of replication obstacles. It is striking that the differences in activity were observed regardless of the type of bulky DNA modification, whether it was within the DNA backbone or on the nucleobases, and regardless of the length of the substrate or the distance the modification was placed from the fork junction. Thus, these differences appear to be intrinsic to the mechanism of enzyme translocation along dsDNA.

The ATP-dependent motor domains of the fork remodelers are evolutionarily related to Snf2 family chromatin remodelers, which translocate along one strand (the “tracking strand”) while also making essential contacts to the non-tracking (or “guide”) strand from the minor groove side of the duplex (13,33-43). HLTF, like the Snf2 translocases, has been shown to have 3′-5′

polarity on the tracking strand, which would place translocation along the lagging strand (13,33,35,44). Therefore, the fact that SMARCAL1 and ZRANB3 are selectively inhibited on the leading strand seems counter-intuitive and could mean that these enzymes translocate on the leading strand with 5′-3′ polarity. However, this interpretation is unlikely given their divergence from known 5′-3′ translocases (45-47). A more plausible interpretation is that SMARCAL1 and ZRANB3 track 3′-5′ along the lagging template strand, while also making intimate contacts to the leading template (guide) strand and/or the minor groove that would render SMARCAL1 and ZRANB3 sensitive to bulky lesions and impede translocation. Indeed, SMARCAL1 and ZRANB3 can be distinguished from HLTF and the other Snf2 family members by the sequences of helicase-related motifs IIa and Vb, which make the contacts to the guide strand and minor groove in dsDNA translocases (13,34,48).

The differences in the ability of the enzymes to work in the presence of leading or lagging strand modifications could also be due to how the substrate recognition domains contact DNA and facilitate the annealing of strands. The substrate recognition domains of SMARCAL1 and ZRANB3 are thought to be similar while the HLTF HIRAN domain is structurally and functionally different. Perhaps the substrate recognition domains of SMARCAL1 and ZRANB3 are inhibited by the leading strand modifications even though the ATPase domains translocate primarily on the lagging strand (13,33,35,44). Both SMARCAL1 and HTLF bind duplex DNA at a model replication fork through their ATPase domains (9,24). However, whereas the HLTF HIRAN domain contacts the nascent strand, the SMARCAL HARP domain contacts the template strands at the fork junction (9). Thus, the leading strand DNA modifications in the template strand may not allow the SMARCAL HARP domain or the SRD in ZRANB3 to make the proper contacts needed for reversal.

Of the three translocases, HLTF appears to be unique in its insensitivity to DNA modifications. This result is consistent with the recent finding that HLTF can resolve G4 structures in DNA (49) and remove Cas9-gRNA complexes (50). HLTF travels on dsDNA and destabilizes the G4 structure through its translocase activity, which both unfolds the G4 structure and promotes reannealing of the structure-forming ssDNA to its complementary strand (49). Thus, HLTF is unique among the ATP-dependent translocases in this regard and may generate more force than SMARCAL1 or ZRANB3 to enable translocation through various impediments. Unlike the HARP domain of SMARCAL1 and the SRD of ZRANB3, the HIRAN domain of HLTF does not make extensive contacts with the ssDNA of the leading template strand. Instead, it binds the 3′ hydroxyl group of the nascent leading strand, perhaps explaining why it is not inhibited by any of the DNA modifications. Further studies are needed to fully elucidate the translocation and reversal mechanisms of these enzymes.

This work enhances our understanding of the biochemical mechanism of fork regression by the ATP-dependent translocases and helps to explain the need for their seemingly redundant activities. While certain characteristics are shared among these Snf2 member translocases, it is apparent that each enzyme contains unique biochemical functions dependent on the substrate and context it encounters. This highlights the requirement for multiple translocases in the cell to efficiently handle different lesions encountered during DNA elongation to maintain genome stability.

Experimental Procedures

Protein purification

FLAG-SMARCAL1 and FLAG-ZRANB3 were purified from baculovirus infected *Sf9* cells. Cell pellets were lysed in lysis buffer (20 mM Tris pH 7.5, 150 mM NaCl, 0.1 mM EDTA, 1 mM DTT, 0.1% Triton-X and protease inhibitors) for 45 min at 4 °C. Lysates were cleared at 25,000 x g for 30 min at 4 °C. Clarified lysates were added to Flag M2 affinity resin and incubated for 2 hr at 4 °C. The lysate was then spun down at 1,200 *x g* for 5 min and washed 1X in lysis buffer, 2X in LiCl buffer (10 mM HEPES pH 7.6, 0.3 M LiCl, 20% glycerol, 0.01% Triton X-100, 1 mM DTT, 1.5 mM $MgCl_2$, protease inhibitors) and 2X in elution buffer (10 mM HEPES pH 7.6, 100 mM KCl, 1.5 mM $MgCl_2$, 10% glycerol, 1 mM DTT). Protein was eluted in elution buffer with 0.25 mg/mL flag peptide at 4 °C for 30 min. Protein was buffer exchanged into elution buffer without flag peptide, concentrated using an Amicon-Ultra 30-kDa concentrator, and stored at -80 °C.

His-MBP-HLTF was purified as previously described (24). Briefly, full-length HLTF was expressed from baculovirus-infected Hi5 insect cells. Cells were harvested 48 hr after infection and lysed in Buffer A (50 mM Tris-HCl, pH 7.5, 500 mM NaCl, 10% glycerol, 0.01% Nonidet P-40 supplemented with protease inhibitors and 20 mM imidazole). The clarified lysate was incubated with Ni-NTA resin and eluted with 300 mM imidazole in Buffer A. The protein sample was incubated with amylose resin in 50 mM Tris-HCl, pH 7.5, 300 mM NaCl, 10% glycerol, and 0.01% Nonidet P-40 and eluted by on-column cleavage by TEV protease at 4 °C. Imidazole was added to a final concentration of 30 mM and repassed through a nickel affinity column. The sample was concentrated using an Amicon Ultra 30 kDa concentrator, buffer exchanged into 50 mM Tris-HCl, pH 7.5, 250 mM NaCl, 20% glycerol, 0.5 mM EDTA, and 1 mM tris(2-carboxyethyl)phosphine (TCEP), and stored at −80 °C.

Generation of fork reversal substrates

Oligonucleotide sequences used to generate all substrates are listed in Table S1. The combination of oligonucleotides annealed to create each substrate are listed in Table S2 and illustrated in Figure S1.

Cy5 labeled substrates: 48Cy5 or 48Cy5Block was annealed with 52, and 50 or 50Cy5Block was annealed with 53 in 1X saline-sodium citrate (SSC) buffer at 95 °C for 3 min and then gradually cooled to room temperature overnight. The annealed products were combined to form no block, lead Cy5, or lag Cy5 substrates and annealed in annealing buffer (25 mM Tris acetate pH 7.5, 5 mM magnesium acetate, 0.1 mg/ml BSA, 2 mM DTT) at 37 °C for 20 min and subsequently cooled to room temperature. The DNA substrates were then PAGE purified, concentrated and stored at −20 °C until further use.

Internal biotin-streptavidin substrates: Oligonucleotides were end-labeled with [γ-^{32}P]-ATP and T4 polynucleotide kinase (NEB) and purified through a G-25 column (GE healthcare). End-labeled lag N42 was annealed with unlabeled lag P62 or lag P62 biotin, and unlabeled lead N42 was annealed with unlabeled lead P62 or lead p62 biotin in 1X saline-sodium citrate (SSC) buffer at 95 °C for 3 min and then gradually cooled to room temperature overnight. The annealed products were combined to form no biotin, lag biotin or lead biotin substrates and annealed in annealing buffer at 37 °C for 20 min and subsequently cooled to room temperature. The DNA substrates were then PAGE purified, concentrated and stored at −20 °C until further use.

HMCES-DPC substrates: Oligonucleotides were end-labeled with [γ-^{32}P]-ATP and T4 polynucleotide kinase (NEB) and purified through a G-25 column (GE healthcare). End-labeled

lag 82 was annealed to unlabeled lag 122 and end-labeled lead 82 was annealed to unlabeled lead 122 in 1X saline-sodium citrate (SSC) buffer at 95 °C for 3 min and then gradually cooled to room temperature overnight. The lag products were further annealed to lead 122 or lead 122 uracil, and the lead products were further annealed to lag 122 or lag 122 uracil in annealing buffer at 37 °C for 20 min and subsequently cooled to room temperature to generate substrates with ssDNA either on the leading or lagging strand (see Table S2). The DNA substrates were then PAGE purified, concentrated and stored at −20 °C until further use.

Fork reversal assays

Fork reversal on a Cy5 labeled substrate was measured as previously described (14) with minor modifications. Assays were performed at 37 °C in buffer containing 40 mM HEPES pH 7.6, either 20 mM KCl (SMARCAL1), 50 mM KCl (HLTF) or 100 mM KCl (ZRANB3), 5 mM $MgCl_2$, 2 mM ATP, 1 mM TCEP, 100 μg/mL BSA and 5 nM DNA fork substrate. Reactions with varying concentration of fork reversal enzyme (0-100 nM) were quenched after 30 min by adding proteinase K (Sigma-Aldrich, St. Louis, MO, USA) to a final concentration of 1 mg/mL and incubating for 10 min. Reactions were brought to 5% glycerol (v/v) prior to electrophoresis on an 8% non-denaturing polyacrylamide gel at 5 W for 2.5 hr. Gels were imaged for Cy5 at 635 nm excitation and 670 nm emission wavelengths on a Typhoon Trio variable mode imager. Band intensities were quantified, and data were plotted using GraphPad Prism v.10.

Fork reversal on streptavidin-biotin substrates was completed by combining 3 nM of the reversal substrates with 12 nM of streptavidin for 10 min at room temperature in reversal buffer (40 mM Tris pH 7.5, 20 mM KCl, 5 mM $MgCl_2$, 2 mM ATP, 0.1 mg/ml BSA, 2 mM DTT). Increasing amounts of reversal enzyme (0-30 nM) was added to initiate the reaction and reactions were incubated at 37 °C. Reactions were quenched after 30 min by adding proteinase K (Sigma-Aldrich, St. Louis, MO, USA) to a final concentration of 1 mg/mL and incubating for 10 min.

Reactions were brought to 5% glycerol (v/v) prior to electrophoresis on an 8% non-denaturing polyacrylamide gel for 60 min at 80V. Gels were dried, exposed to a phosphor screen and imaged on a Typhoon (Cytiva). Band intensities were quantified, and data were plotted using GraphPad Prism v.10.

For reversal on HMCES-DPC substrates first required crosslinking of HMCES to the abasic site. The reversal substrates were incubated with uracil DNA glycosylase (UDG)(NEB) in fork reversal buffer for 30 min at room temperature to generate an AP site. HMCES was then added in 20-fold excess to the DNA and further incubated for 30 min at room temperature. 1 nM of the HMCES-DPC substrate was then used for fork reversal assays. These assays were carried out in reversal buffer and increasing amounts of enzyme (0-30 nM) at 30 °C. Reactions were quenched after 30 min by adding proteinase K (Sigma-Aldrich, St. Louis, MO, USA) to a final concentration of 1 mg/mL and incubating for 10 min. To test progression on an abasic site alone, a reaction was set up in the absence of HMCES. To test if a proteolyzed HMCES DPC would impede translocation, the HMCES DPC was formed on ssDNA and proteinase K was added for 10 min before annealing to the complementary substrate. The peptide adduct on ssDNA was then annealed and purified as above and used in the fork reversal reaction. Reactions were brought to 5% glycerol (v/v) prior to electrophoresis on an 8% non-denaturing polyacrylamide gel for 60 min at 80V. Gels were dried, exposed to a phosphoscreen and imaged on a Typhoon (Cytiva). Band intensities were quantified, and data were plotted using GraphPad Prism v.10.

Electrophoretic mobility shift assays (EMSA)

For the gel mobility shift assay, increasing concentrations of purified SMARCAL1 and ZRANB3 (0, 10, 50, 100 nM final concentrations) were combined with radiolabeled model fork substrates (1 nM final concentration) in binding buffer (40 mM Tris pH 7.5, 20 mM KCl, 5 mM $MgCl_2$, 0.1

mg/ml BSA, 2 mM DTT) for 15 min at room temperature. Reactions were brought to 5% glycerol (v/v) prior to electrophoresis on an 8% non-denaturing polyacrylamide gel for 60 min at 80 V. Gels were dried, exposed to a phosphoscreen and imaged on a Typhoon (Cytiva). Band intensities were quantified, and data were plotted using GraphPad Prism v.10.

Data availability

All data is available in the article.

Supporting Information

The article contains three supplemental figures and two supplemental tables.

Funding

This work was supported by NIH grants R01GM116616 (DC), R35GM136401 (BFE), R01 GM117299 (BFE), and P01CA092584 (DC, BFE).

Conflict of Interest

The authors declare that they have no conflicts of interest with the contents of this article.

References

1. Zeman, M. K., and Cimprich, K. A. (2014) Causes and consequences of replication stress. *Nature cell biology* **16**, 2-9
2. Cortez, D. (2019) Replication-Coupled DNA Repair. *Mol Cell* **74**, 866-876
3. Saldivar, J. C., Cortez, D., and Cimprich, K. A. (2017) The essential kinase ATR: ensuring faithful duplication of a challenging genome. *Nature reviews. Molecular cell biology* **18**, 622-636
4. Conti, B. A., and Smogorzewska, A. (2020) Mechanisms of direct replication restart at stressed replisomes. *DNA Repair (Amst)* **95**, 102947
5. Joseph, S. A., Taglialatela, A., Leuzzi, G., Huang, J. W., Cuella-Martin, R., and Ciccia, A. (2020) Time for remodeling: SNF2-family DNA translocases in replication fork metabolism and human disease. *DNA Repair (Amst)* **95**, 102943
6. Eichman, B. F. (2023) Repair and tolerance of DNA damage at the replication fork: A structural perspective. *Curr Opin Struct Biol* **81**, 102618
7. Adolph, M. B., and Cortez, D. (2024) Mechanisms and regulation of replication fork reversal. *DNA Repair (Amst)* **141**, 103731
8. Neelsen, K. J., and Lopes, M. (2015) Replication fork reversal in eukaryotes: from dead end to dynamic response. *Nature Reviews Molecular Cell Biology* **16**, 207-220
9. Betous, R., Mason, A. C., Rambo, R. P., Bansbach, C. E., Badu-Nkansah, A., Sirbu, B. M., Eichman, B. F., and Cortez, D. (2012) SMARCAL1 catalyzes fork regression and Holliday junction migration to maintain genome stability during DNA replication. *Genes Dev* **26**, 151-162
10. Vujanovic, M., Krietsch, J., Raso, M. C., Terraneo, N., Zellweger, R., Schmid, J. A., Taglialatela, A., Huang, J. W., Holland, C. L., Zwicky, K., Herrador, R., Jacobs, H., Cortez, D., Ciccia, A., Penengo, L., and Lopes, M. (2017) Replication Fork Slowing and

Reversal upon DNA Damage Require PCNA Polyubiquitination and ZRANB3 DNA Translocase Activity. *Mol Cell* **67**, 882-890 e885

11. Kile, A. C., Chavez, D. A., Bacal, J., Eldirany, S., Korzhnev, D. M., Bezsonova, I., Eichman, B. F., and Cimprich, K. A. (2015) HLTF's Ancient HIRAN Domain Binds 3' DNA Ends to Drive Replication Fork Reversal. *Mol Cell* **58**, 1090-1100
12. Ciccia, A., Nimonkar, A. V., Hu, Y., Hajdu, I., Achar, Y. J., Izhar, L., Petit, S. A., Adamson, B., Yoon, J. C., Kowalczykowski, S. C., Livingston, D. M., Haracska, L., and Elledge, S. J. (2012) Polyubiquitinated PCNA recruits the ZRANB3 translocase to maintain genomic integrity after replication stress. *Mol Cell* **47**, 396-409
13. Dürr, H., Flaus, A., Owen-Hughes, T., and Hopfner, K. P. (2006) Snf2 family ATPases and DExx box helicases: differences and unifying concepts from high-resolution crystal structures. *Nucleic Acids Res* **34**, 4160-4167
14. Mason, A. C., Rambo, R. P., Greer, B., Pritchett, M., Tainer, J. A., Cortez, D., and Eichman, B. F. (2014) A structure-specific nucleic acid-binding domain conserved among DNA repair proteins. *Proc Natl Acad Sci U S A* **111**, 7618-7623
15. Badu-Nkansah, A., Mason, A. C., Eichman, B. F., and Cortez, D. (2016) Identification of a Substrate Recognition Domain in the Replication Stress Response Protein Zinc Finger Ran-binding Domain-containing Protein 3 (ZRANB3). *J Biol Chem* **291**, 8251-8257
16. Bansbach, C. E., Betous, R., Lovejoy, C. A., Glick, G. G., and Cortez, D. (2009) The annealing helicase SMARCAL1 maintains genome integrity at stalled replication forks. *Genes Dev* **23**, 2405-2414
17. Yuan, J., Ghosal, G., and Chen, J. (2009) The annealing helicase HARP protects stalled replication forks. *Genes Dev* **23**, 2394-2399
18. Ciccia, A., Bredemeyer, A. L., Sowa, M. E., Terret, M. E., Jallepalli, P. V., Harper, J. W., and Elledge, S. J. (2009) The SIOD disorder protein SMARCAL1 is an RPA-interacting protein involved in replication fork restart. *Genes Dev* **23**, 2415-2425

19. Yusufzai, T., Kong, X., Yokomori, K., and Kadonaga, J. T. (2009) The annealing helicase HARP is recruited to DNA repair sites via an interaction with RPA. *Genes Dev* **23**, 2400-2404

20. Postow, L., Woo, E. M., Chait, B. T., and Funabiki, H. (2009) Identification of SMARCAL1 as a component of the DNA damage response. *J Biol Chem* **284**, 35951-35961

21. Yuan, J., Ghosal, G., and Chen, J. (2012) The HARP-like domain-containing protein AH2/ZRANB3 binds to PCNA and participates in cellular response to replication stress. *Mol Cell* **47**, 410-421

22. Betous, R., Couch, F. B., Mason, A. C., Eichman, B. F., Manosas, M., and Cortez, D. (2013) Substrate-selective repair and restart of replication forks by DNA translocases. *Cell Rep* **3**, 1958-1969

23. Bhat, K. P., Betous, R., and Cortez, D. (2015) High-affinity DNA-binding domains of replication protein A (RPA) direct SMARCAL1-dependent replication fork remodeling. *J Biol Chem* **290**, 4110-4117

24. Chavez, D. A., Greer, B. H., and Eichman, B. F. (2018) The HIRAN domain of helicase-like transcription factor positions the DNA translocase motor to drive efficient DNA fork regression. *J Biol Chem* **293**, 8484-8494

25. Hishiki, A., Sato, M., and Hashimoto, H. (2020) Structure of HIRAN domain of human HLTF bound to duplex DNA provides structural basis for DNA unwinding to initiate replication fork regression. *J Biochem* **167**, 597-602

26. Achar, Y. J., Balogh, D., Neculai, D., Juhasz, S., Morocz, M., Gali, H., Dhe-Paganon, S., Venclovas, C., and Haracska, L. (2015) Human HLTF mediates postreplication repair by its HIRAN domain-dependent replication fork remodelling. *Nucleic Acids Res* **43**, 10277-10291

27. Mohni, K. N., Wessel, S. R., Zhao, R., Wojciechowski, A. C., Luzwick, J. W., Layden, H., Eichman, B. F., Thompson, P. S., Mehta, K. P. M., and Cortez, D. (2019) HMCES Maintains Genome Integrity by Shielding Abasic Sites in Single-Strand DNA. *Cell* **176**, 144-153 e113

28. Thompson, P. S., Amidon, K. M., Mohni, K. N., Cortez, D., and Eichman, B. F. (2019) Protection of abasic sites during DNA replication by a stable thiazolidine protein-DNA cross-link. *Nat Struct Mol Biol* **26**, 613-618

29. Halabelian, L., Ravichandran, M., Li, Y., Zeng, H., Rao, A., Aravind, L., and Arrowsmith, C. H. (2019) Structural basis of HMCES interactions with abasic DNA and multivalent substrate recognition. *Nat Struct Mol Biol* **26**, 607-612

30. Wang, N., Bao, H., Chen, L., Liu, Y., Li, Y., Wu, B., and Huang, H. (2019) Molecular basis of abasic site sensing in single-stranded DNA by the SRAP domain of E. coli yedK. *Nucleic Acids Res* **47**, 10388-10399

31. Rua-Fernandez, J., Lovejoy, C. A., Mehta, K. P. M., Paulin, K. A., Toudji, Y. T., Giansanti, C., Eichman, B. F., and Cortez, D. (2023) Self-reversal facilitates the resolution of HMCES DNA-protein crosslinks in cells. *Cell reports* **42**, 113427

32. Donsbach, M., Durauer, S., Grunert, F., Nguyen, K. T., Nigam, R., Yaneva, D., Weickert, P., Bezalel-Buch, R., Semlow, D. R., and Stingele, J. (2023) A non-proteolytic release mechanism for HMCES-DNA-protein crosslinks. *EMBO J* **42**, e113360

33. Whitehouse, I., Stockdale, C., Flaus, A., Szczelkun, M. D., and Owen-Hughes, T. (2003) Evidence for DNA translocation by the ISWI chromatin-remodeling enzyme. *Mol Cell Biol* **23**, 1935-1945

34. Dürr, H., Körner, C., Müller, M., Hickmann, V., and Hopfner, K. P. (2005) X-ray structures of the Sulfolobus solfataricus SWI2/SNF2 ATPase core and its complex with DNA. *Cell* **121**, 363-373

35. Saha, A., Wittmeyer, J., and Cairns, B. R. (2005) Chromatin remodeling through directional DNA translocation from an internal nucleosomal site. *Nat Struct Mol Biol* **12**, 747-755

36. Farnung, L., Vos, S. M., Wigge, C., and Cramer, P. (2017) Nucleosome-Chd1 structure and implications for chromatin remodelling. *Nature* **550**, 539-542

37. Liu, X., Li, M., Xia, X., Li, X., and Chen, Z. (2017) Mechanism of chromatin remodelling revealed by the Snf2-nucleosome structure. *Nature* **544**, 440-445

38. Aramayo, R. J., Willhoft, O., Ayala, R., Bythell-Douglas, R., Wigley, D. B., and Zhang, X. (2018) Cryo-EM structures of the human INO80 chromatin-remodeling complex. *Nat Struct Mol Biol* **25**, 37-44

39. Ayala, R., Willhoft, O., Aramayo, R. J., Wilkinson, M., McCormack, E. A., Ocloo, L., Wigley, D. B., and Zhang, X. (2018) Structure and regulation of the human INO80-nucleosome complex. *Nature* **556**, 391-395

40. Willhoft, O., Ghoneim, M., Lin, C. L., Chua, E. Y. D., Wilkinson, M., Chaban, Y., Ayala, R., McCormack, E. A., Ocloo, L., Rueda, D. S., and Wigley, D. B. (2018) Structure and dynamics of the yeast SWR1-nucleosome complex. *Science* **362**

41. Li, M., Xia, X., Tian, Y., Jia, Q., Liu, X., Lu, Y., Li, M., Li, X., and Chen, Z. (2019) Mechanism of DNA translocation underlying chromatin remodelling by Snf2. *Nature* **567**, 409-413

42. Yan, L., Wu, H., Li, X., Gao, N., and Chen, Z. (2019) Structures of the ISWI–nucleosome complex reveal a conserved mechanism of chromatin remodeling. *Nature Structural & Molecular Biology* **26**, 258-266

43. Nodelman, I. M., Das, S., Faustino, A. M., Fried, S. D., Bowman, G. D., and Armache, J.-P. (2022) Nucleosome recognition and DNA distortion by the Chd1 remodeler in a nucleotide-free state. *Nature Structural & Molecular Biology* **29**, 121-129

44. Blastyák, A., Hajdú, I., Unk, I., and Haracska, L. (2010) Role of double-stranded DNA translocase activity of human HLTF in replication of damaged DNA. *Mol Cell Biol* **30**, 684-693

45. Singleton, M. R., Dillingham, M. S., and Wigley, D. B. (2007) Structure and mechanism of helicases and nucleic acid translocases. *Annu Rev Biochem* **76**, 23-50

46. Kuper, J., Wolski, S. C., Michels, G., and Kisker, C. (2012) Functional and structural studies of the nucleotide excision repair helicase XPD suggest a polarity for DNA translocation. *Embo j* **31**, 494-502

47. Cheng, K., and Wigley, D. B. (2018) DNA translocation mechanism of an XPD family helicase. *Elife* **7**

48. Fairman-Williams, M. E., Guenther, U. P., and Jankowsky, E. (2010) SF1 and SF2 helicases: family matters. *Curr Opin Struct Biol* **20**, 313-324

49. Bai, G., Endres, T., Kuhbacher, U., Mengoli, V., Greer, B. H., Peacock, E. M., Newton, M. D., Stanage, T., Dello Stritto, M. R., Lungu, R., Crossley, M. P., Sathirachinda, A., Cortez, D., Boulton, S. J., Cejka, P., Eichman, B. F., and Cimprich, K. A. (2024) HLTF resolves G4s and promotes G4-induced replication fork slowing to maintain genome stability. *Mol Cell* **84**, 3044-3060 e3011

50. Reginato, G., Dello Stritto, M. R., Wang, Y., Hao, J., Pavani, R., Schmitz, M., Halder, S., Morin, V., Cannavo, E., Ceppi, I., Braunshier, S., Acharya, A., Ropars, V., Charbonnier, J. B., Jinek, M., Nussenzweig, A., Ha, T., and Cejka, P. (2024) HLTF disrupts Cas9-DNA post-cleavage complexes to allow DNA break processing. *Nat Commun* **15**, 5789

Abbreviations

AP, abasic site; DPC, DNA protein crosslink; TLS, translesion synthesis; dsDNA, double-stranded DNA; ssDNA, single-stranded DNA; RPA, replication protein A; SMARCAL1, SWI/SNF-related matrix-associated actin-dependent regulator of chromatin subfamily A-like protein 1; ZRANB3, Zinc finger Ran-binding domain-containing protein 3; HLTF, Helicase-like transcription factor; Snf2, sucrose non-fermenter 2; SRD, substrate recognition domain; HMCES, Embryonic stem cell-specific 5-hydroxymethylcytosine-binding protein, ES cell-specific 5hmC-binding protein; BSA, bovine serum albumin

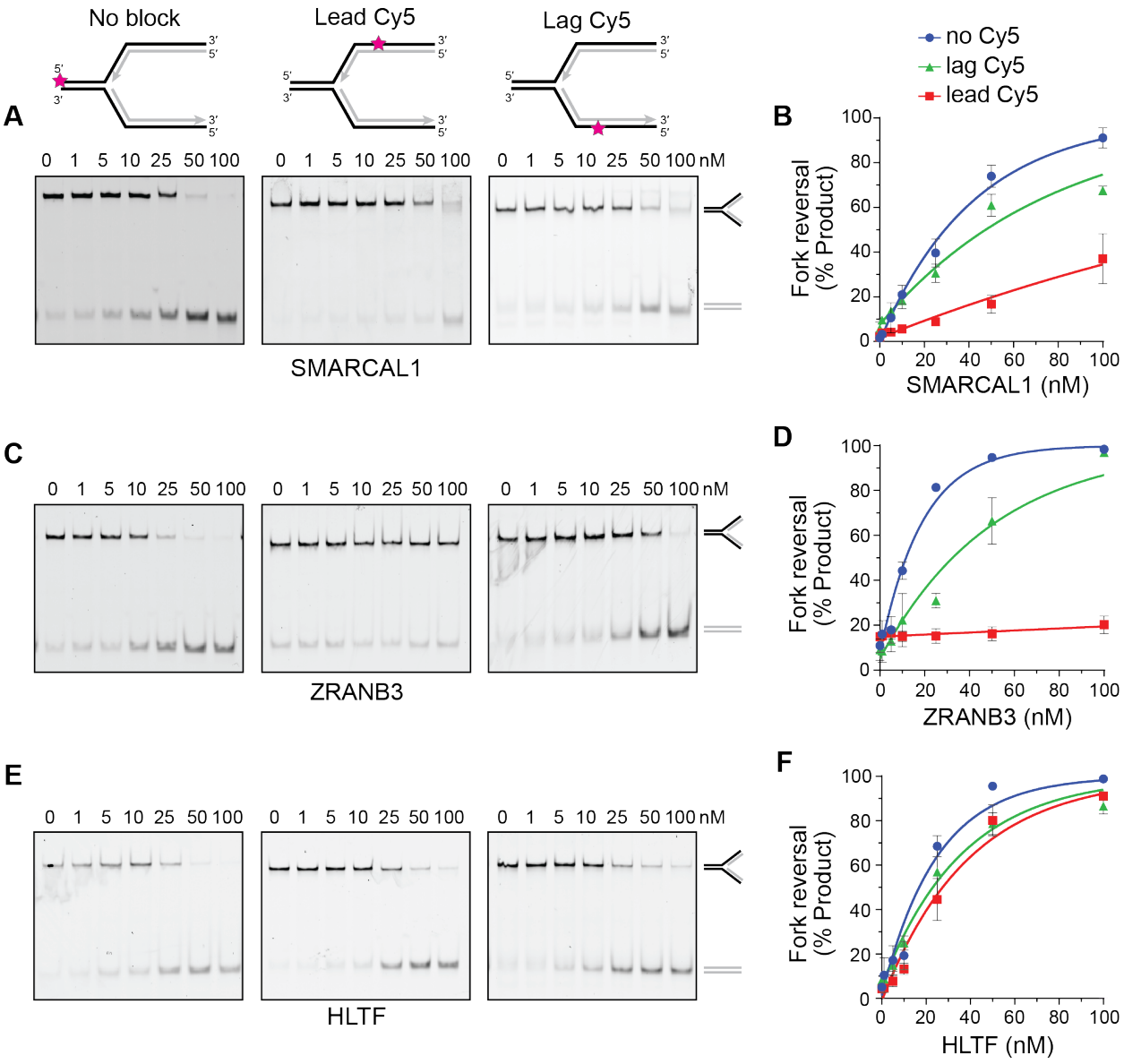

Figure 1. Fork reversal on model replication substrates containing a Cy5 lesion. (A, C, E) Representative native PAGE gels for fork reversal assays performed with (A) SMARCAL1, (C) ZRANB3, or (E) HLTF on an unmodified DNA fork, a leading template Cy5 lesion, or a lagging template Cy5 lesion. DNA substrates used in fork reversal activity assays are shown with the Cy5 location labeled by a star (magenta). (B, D, F) Quantification of fork reversal assays performed in triplicate for (A) SMARCAL1, (C) ZRANB3, or (E) HLTF.

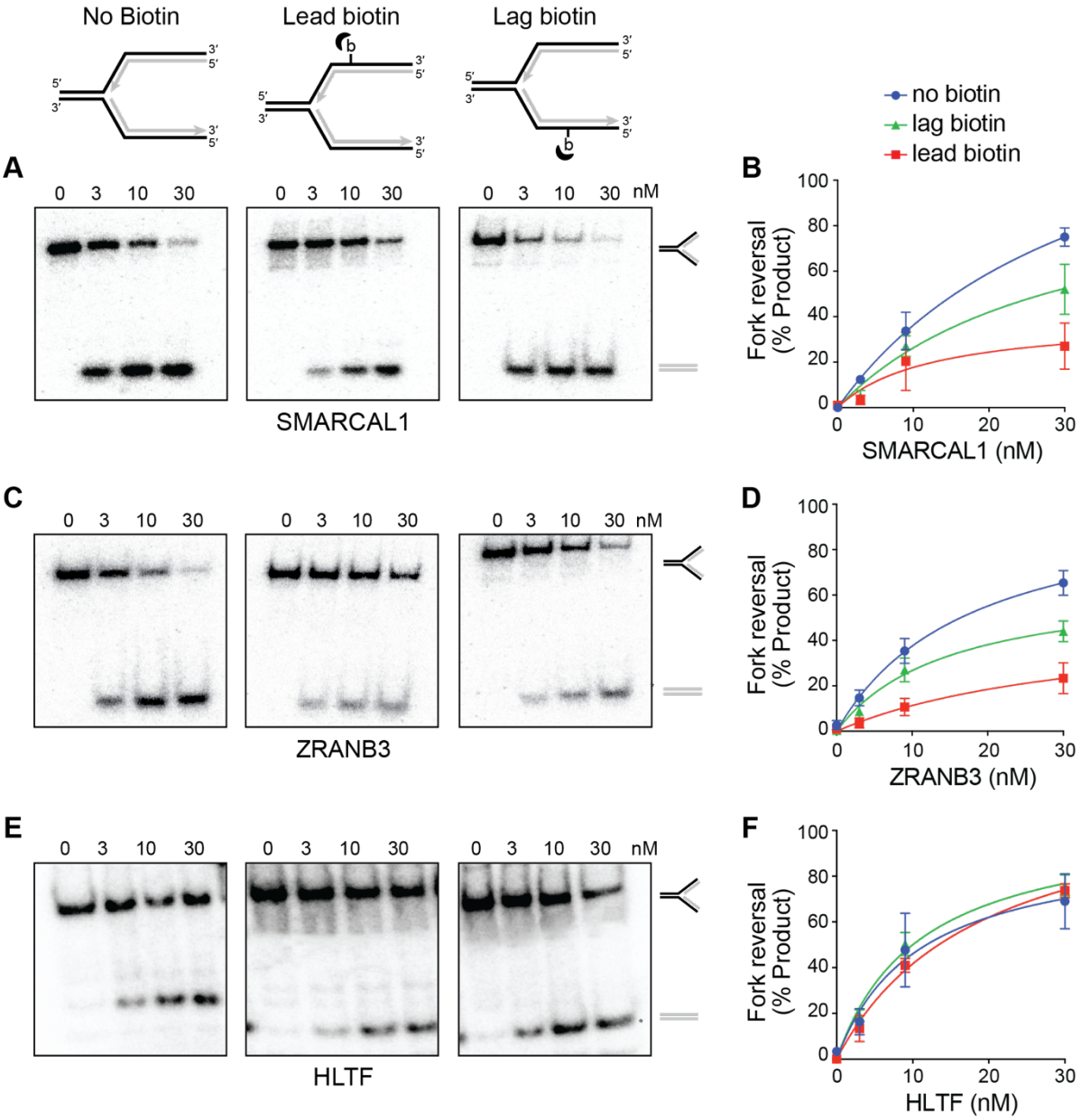

Figure 2. **Fork reversal on model replication substrates containing a streptavidin-biotin lesion.** (A, C, E) Representative native PAGE gels for fork reversal assays performed with (A) SMARCAL1, (C) ZRANB3, or (E) HLTF on an unmodified DNA fork, a leading template biotin-streptavidin lesion, or a lagging template biotin-streptavidin lesion. DNA substrates used in fork reversal activity assays are shown with location of the biotin-streptavidin. (B, D, F)

Quantification of fork reversal assays performed in triplicate for (A) SMARCAL1, (C) ZRANB3, or (E) HLTF.

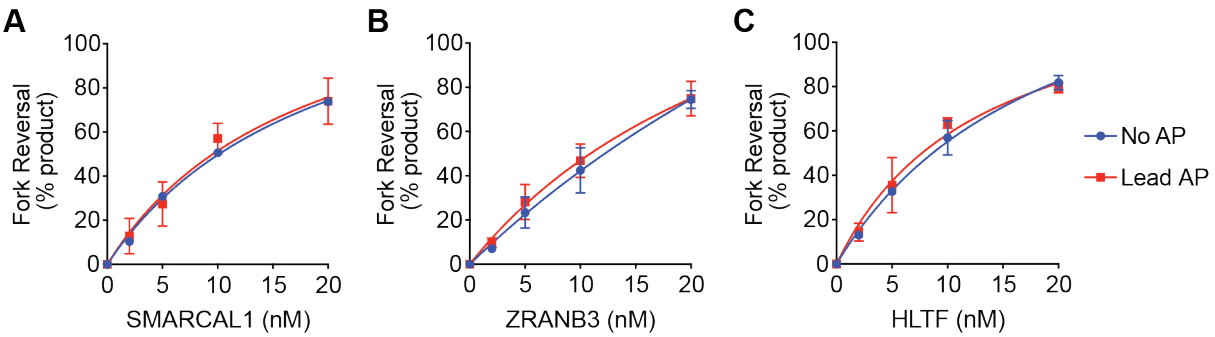

Figure 3. Fork reversal on model replication substrate containing an AP site. Quantitation of fork reversal by (A) SMARCAL1, (B) ZRANB3, or (C) HLTF in the presence of a leading strand abasic site.

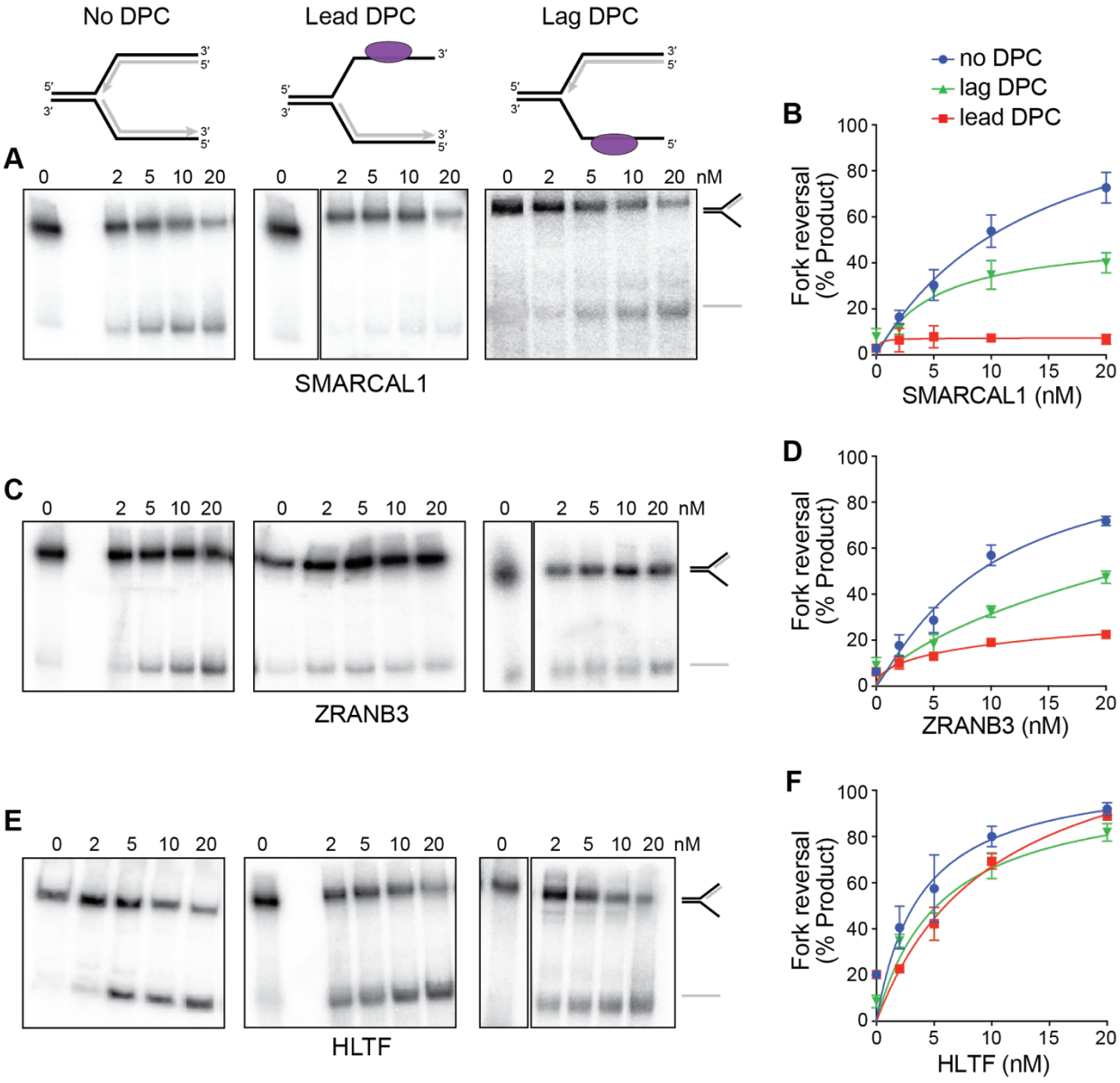

Figure 4. **Fork reversal on model replication substrates containing a HMCES-DPC.** (A, C, E) Representative native PAGE gels for fork reversal assays performed with (A) SMARCAL1, (C) ZRANB3, or (E) HLTF on an unmodified DNA fork, a leading template HMCES-DPC lesion, or a lagging template HMCES-DPC lesion. DNA substrates used in fork reversal activity assays are shown with location of the HMCES-DPC. (B, D, F) Quantification of fork reversal assays performed in triplicate for (A) SMARCAL1, (C) ZRANB3, or (E) HLTF.